PNAS RESEARCH ARTICLE | PLANT BIOLOGY

Targeted engineering of camelina and pennycress seeds for ultrahigh accumulation of acetyl-TAG

Linah Alkotami[a], Dexter J. White[a], Kathleen M. Schuler[b], Maliheh Esfahanian[c], Brice A. Jarvis[c], Andrew E. Paulson[d], Somnath Koley[e], Jinling Kang[f], Chaofu Lu[f], Doug K. Allen[e,g], Young-Jin Lee[d], John C. Sedbrook[c], and Timothy P. Durrett[a,1]

Affiliations are included on p. 9.

Edited by Clinton Chapple, Purdue University, West Lafayette, IN; received June 24, 2024; accepted October 4, 2024

Acetyl-TAG (3-acetyl-1,2-diacylglycerol), unique triacylglycerols (TAG) possessing an acetate group at the *sn*-3 position, exhibit valuable properties, such as reduced viscosity and freezing points. Previous attempts to engineer acetyl-TAG production in oilseed crops did not achieve the high levels found in naturally producing *Euonymus* seeds. Here, we demonstrate the successful generation of camelina and pennycress transgenic lines accumulating nearly pure acetyl-TAG at 93 mol% and 98 mol%, respectively. These ultrahigh acetyl-TAG synthesizing lines were created using gene-edited *FATTY ACID ELONGASE1* (*FAE1*) mutant lines as an improved genetic background to increase levels of acetyl-CoA available for acetyl-TAG synthesis mediated by the expression of EfDAcT, a high-activity diacylglycerol acetyltransferase isolated from *Euonymus fortunei*. Combining EfDAcT expression with suppression of the competing TAG-synthesizing enzyme DGAT1 further enhanced acetyl-TAG accumulation. These ultrahigh levels of acetyl-TAG exceed those in earlier engineered oilseeds and are equivalent or greater than those in *Euonymus* seeds. Imaging of lipid localization in transgenic seeds revealed that the low amounts of residual TAG were mostly confined to the embryonic axis. Similar spatial distributions of specific TAG and acetyl-TAG molecular species, as well as their probable diacylglycerol (DAG) precursors, provide additional evidence that acetyl-TAG and TAG are both synthesized from the same tissue-specific DAG pools. Remarkably, this ultrahigh production of acetyl-TAG in transgenic seeds exhibited minimal negative effects on seed properties, highlighting the potential for production of designer oils required for economical biofuel industries.

biofuels | oil seeds | synthetic biology | triacylglycerols

Significance

Many nonagronomic plants produce unusual triacylglycerols in their seed oil possessing different functionalities, making them useful for industrial applications. Metabolically engineering oil seed crops to produce high levels of desirable lipid profiles, comparable to those found in natural species, has proven challenging. Here, by altering key endogenous lipid pathways and expressing a high-activity acetyl-transferase from *Euonymus fortunei*, we successfully remodeled triacylglycerol synthesis in the emerging oilseed crops camelina and pennycress. These targeted modifications resulted in seeds with almost pure levels of 3-acetyl-1,2-diacylglycerols, unusual lipids with reduced viscosity, and improved cold temperature properties with potential as an improved diesel replacement. Our results demonstrate the feasibility of engineering designer lipids with extreme lipid compositions for sustainable plant-based fuels.

Euonymus species naturally accumulate more than 90% of 3-acetyl-1,2-diacylglycerol (acetyl-TAG) in their seeds as the major form of lipid storage (1, 2). The *sn*-3 acetate group imparts altered physical and chemical properties to the resulting oil, such as reduced kinematic viscosity and lower freezing temperatures, expanding its applicability for industrial and biofuel uses (3, 4). While species like *Euonymus* that synthesize unusual oils often possess poor agronomic traits that prevent them from being cultivated as crops, their specific enzymatic machinery responsible for synthesizing these atypical triacylglycerols (TAG) can be harnessed to engineer oilseed crops with tailored oil profiles. Camelina (*Camelina sativa* L.) and pennycress (*Thlaspi arvense* L.) have emerged as promising candidates for such genetic engineering efforts due to their short life cycle, amenable agronomic traits, and well-established transformation protocols facilitating efficient genetic modifications (5–7).

Acetyl-TAG are synthesized by diacylglycerol acetyltransferases (DAcT), enzymes that utilize diacylglycerol (DAG) and acetyl-CoA substrates to synthesize acetyl-TAG (3, 8). Heterologous expression of the EaDAcT enzyme isolated from *Euonymus alatus* resulted in the synthesis of acetyl-TAG in different oilseed crops, albeit achieving only 55 to 70 mol% in the best transgenic seeds (4, 7, 9). Suppressing *DIACYLGLYCEROL ACYLTRANSFERASE1* (*DGAT1*), which catalyzes the final step of endogenous TAG synthesis, further enhanced acetyl-TAG production (4, 9, 10). In addition, *DGAT1* suppression coupled with the expression of the higher activity EfDAcT enzyme from *Euonymus fortunei* resulted in transgenic camelina lines accumulating up to 87 mol% acetyl-TAG (10). Despite these efforts, acetyl-TAG levels in transgenic camelina and pennycress remained below those naturally produced in *Euonymus* seeds.

In oilseeds, particularly those of the Brassicaceae, the acetyl-CoA substrate used by DAcT to produce acetyl-TAG is also utilized by the fatty acid elongase complex to elongate oleic acid (18:1) to very-long-chain fatty acids (VLCFAs) such as gondoic acid (20:1) and erucic acid (22:1) (11, 12). Thus, eliminating fatty acid elongation, for example, by

Author contributions: L.A., D.J.W., Y.-J.L., J.C.S., and T.P.D. designed research; L.A., D.J.W., K.M.S., M.E., B.A.J., A.E.P., and S.K. performed research; J.K. and C.L. contributed new reagents/analytic tools; L.A., D.J.W., K.M.S., M.E., B.A.J., A.E.P., S.K., D.K.A., Y.-J.L., J.C.S., and T.P.D. analyzed data; and L.A. and T.P.D. wrote the paper.

The authors declare no competing interest.

This article is a PNAS Direct Submission.

[1]To whom correspondence may be addressed. Email: tdurrett@ksu.edu.

This article contains supporting information online at https://www.pnas.org/lookup/suppl/doi:10.1073/pnas.2412542121/-/DCSupplemental.

Published November 11, 2024.

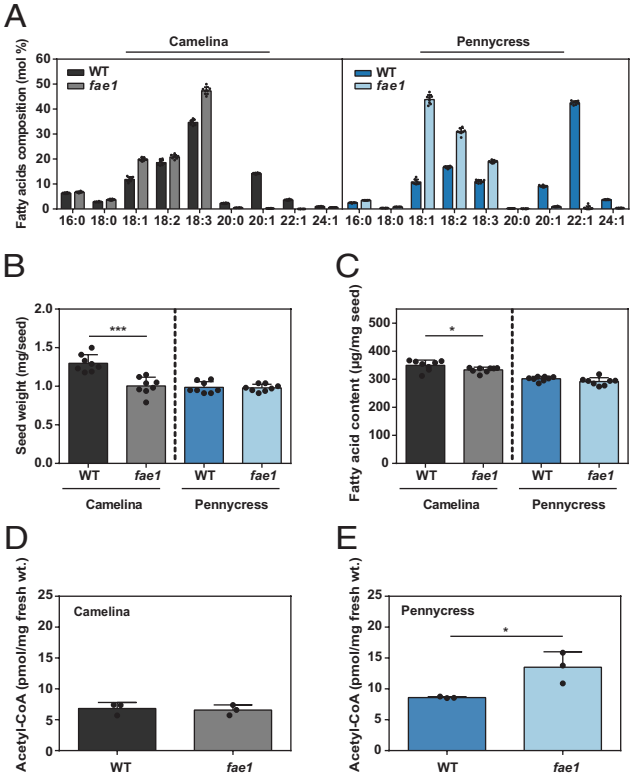

Fig. 1. Pennycress *fae1* mutant seeds possess increased levels of acetyl-CoA. Seed fatty acid composition (*A*), seed weight (*B*), seed fatty acid content (*C*), and seed acetyl-CoA levels (*D* and *E*) of camelina and pennycress wild-type and *fae1* mutant seed. Data represent mean ± SE, n ≥ 3 biological replicates. Asterisks indicate statistical difference from wild-type seeds (Student's *t* test; $*P \leq 0.05$, $***P \leq 0.001$).

mutating the *FATTY ACID ELONGASE1* (*FAE1*) gene, could make more acetyl-CoA available for synthesis of acetyl-TAG. In this study, we utilized camelina and pennycress *fae1* mutants as a platform to further elevate acetyl-TAG production. By genetically fine-tuning the fatty acid composition and availability of DAG substrate in the plant background used to produce acetyl-TAG, we document near-quantitative remodeling of the endogenous TAG profile, resulting in a high-value oil with immediate applications in industry.

Results

Pennycress *fae1* Seeds Possess Elevated Levels of Acetyl-CoA. We hypothesized that seeds with *fae1* mutations would have higher levels of acetyl-CoA, creating a more favorable environment for EfDAcT acetyltransferase activity and ultimately leading to a greater accumulation of acetyl-TAG. To assess our hypothesis, we characterized *fae1* knockout mutant lines of camelina (13) and pennycress (7), two emerging oilseed crops that produce different amounts of VLCFA, with pennycress accumulating 58 mol% of fatty acids 20 carbons or longer, much higher than the 26 mol% observed in camelina (Fig. 1*A*). Mutant *fae1* seeds of both camelina and pennycress contained small amounts of VLCFA (<2%) and increased levels of 18:1, 18:2, and 18:3 fatty acids (Fig. 1*A*). Interestingly, the proportions of these fatty acids differed between the two species. In camelina *fae1* mutants, the major fatty acid is 18:3, mirroring the wild-type background, whereas pennycress *fae1* mutants primarily accumulated 18:1 as their major fatty acid (Fig. 1*A*). The average weight and fatty acid content of camelina *fae1* seed was slightly decreased compared to wild-type seeds (Fig. 1 *B* and *C*). In contrast, both the average weight and fatty acid content of pennycress *fae1* seeds were similar to those of the wild-type (Fig. 1 *B* and *C*). Consistent with the relatively low amounts of VLCFA in camelina wild-type seeds, acetyl-CoA levels in developing camelina *fae1* seeds were not significantly different from that of the wild-type seeds (Fig. 1*D*). However, an increase of 57% of acetyl-CoA levels was observed in developing pennycress *fae1* seeds compared to the wild-type controls (Fig. 1*E*).

Camelina *fae1* Mutation Slightly Increases Acetyl-TAG Accumulation. To test the impact of the *fae1* mutation on acetyl-TAG accumulation in camelina, *EfDAcT* was expressed in *fae1* mutant seeds, either alone or in combination with *DGAT1* RNA interference (RNAi). On average, acetyl-TAG content in *fae1* T2 seeds segregating for *EfDAcT* was 75 mol% (Fig. 2*A*), higher than the 71 mol% previously observed in seeds with a wild-type background (10). Likewise, expression of *EfDAcT+DGAT1 RNAi* resulted in an average accumulation of 87 mol% acetyl-TAG in *fae1* seeds, compared to 80 mol% in wild-type seeds (Fig. 2*A*).

The two highest acetyl-TAG-producing lines from each genotype were then grown together to directly compare acetyl-TAG accumulation. *EfDAcT* homozygous lines in a *fae1* background accumulated 88 mol% acetyl-TAG, higher than the 81 mol% of acetyl-TAG observed on average in a wild-type background (Fig. 2*B*). However, *EfDAcT+DGAT1 RNAi* homozygous *fae1* lines accumulated on average 90 mol% of acetyl-TAG, reaching up to 93 mol% in the highest line, almost identical to the levels observed in the homozygous *EfDAcT+DGAT1 RNAi* lines in wild-type background (Fig. 2*B*). Analysis of TAG fatty acid composition of *EfDAcT* and *EfDAcT+DGAT1 RNAi* transgenic lines revealed higher levels of 18:2 and lower levels of 18:3 and 20:1 compared to wild-type seeds (*SI Appendix*, Fig. S1*A*). Similar to previous results (10), VLCFAs 20:0 and 22:1 were mainly present in the TAG fraction of the transgenic lines (*SI Appendix*, Fig. S1*A*). Transgenic seeds in the *fae1* background contained higher levels of 18:2 and lower levels of 18:3 (*SI Appendix*, Fig. S1*B*).

To better compare the impact of mutating *fae1* on acetyl-TAG production without the confounding effect of different transgenic loci possessing varying levels of expression, we crossed high acetyl-TAG-producing lines expressing either *EfDAcT* or *EfDAcT+DGAT1 RNAi* in a wild-type background into the *fae1* mutant line. Because camelina possesses three active *FAE1* homeologs (13, 14), identification of transgenic lines in a triple *fae1* mutant background from a segregating backcross population would be particularly onerous. Instead, we measured acetyl-TAG and 20:1 levels in individual transgenic seeds derived from segregating F2 backcross populations. Here, transgenic *EfDAcT* F2 seed possessed a low negative correlation between acetyl-TAG accumulation and 20:1 levels (Fig. 2*C*). The seed with the lowest 20:1 level (4.4 mol%) possessed the highest levels of acetyl-TAG (84 mol%), greater than the 76 mol% observed in seed from the parental *EfDAcT* line (Fig. 2*C*). In contrast, transgenic seeds from the *fae1* x *EfDAcT+DGAT1 RNAi* F2 cross, showed no correlation between acetyl-TAG and 20:1 levels (Fig. 2*D*).

Transgenic *fae1* Pennycress Seeds Accumulate up to 98 Mol% of Acetyl-TAG. Given the increased acetyl-CoA levels in pennycress *fae1* seeds (Fig. 1*E*), we generated stable transgenic pennycress lines in both wild-type and *fae1* backgrounds expressing *EfDAcT* with and without *DGAT1 RNAi* (*SI Appendix*, Fig. S2*A*). For each genotype, the three independent lines exhibiting the highest acetyl-TAG levels were selected for further propagation (*SI Appendix*, Fig. S2*B*). In accordance with our hypothesis, acetyl-TAG levels were significantly higher in the *fae1* mutant background (Fig. 3*A*). For example, expression of *EfDAcT* in *fae1* seeds resulted in an

average of 95 mol% of acetyl-TAG, compared to only 48 mol% in the wild-type background. Similarly, expression of *EfDAcT+DGAT1 RNAi* in *fae1* seeds resulted in an average acetyl-TAG accumulation of 96 mol%, higher than the 79 mol% accumulation observed in the wild-type background. Importantly, acetyl-TAG levels were 98 mol% in the best *EfDAcT+DGAT1 RNAi* transgenic line in the *fae1* background (Fig. 3*A*), exceeding the naturally occurring levels produced by many *Euonymus* seeds (1, 3).

The ultrahigh levels of acetyl-TAG in the *fae1* background were further confirmed by electrospray ionization mass spectrometry (ESI-MS). Trace amounts of TAG in the *fae1* background, less than 4% and 1% of total signal intensity, were observed in *EfDAcT* and *EfDAcT+DGAT1 RNAi* seeds, respectively (Fig. 3*B* and *SI Appendix*, Fig. S3). Most of the residual TAG molecular species in *EfDAcT+DGAT1 RNAi* seeds possessed 54 carbons (Fig. 3*B*), while in *EfDAcT* transgenic seed, TAG molecular species were similar to those found in nontransgenic *fae1* seed, being dominated by molecular species with 54 carbons, but also possessing molecular species containing VLCFA (*SI Appendix*, Fig. S3). Seeds in the wild-type background possessed a more complicated molecular species profile for both acetyl-TAG and TAG, reflective of the ability to synthesize high levels of VLCFA. These ESI-MS results were also reflected in fatty acid analysis of the seeds, where total TAG in transgenic seeds in the wild-type background possessed significantly lower accumulation of 22:1 and higher accumulation of 18:1 (*SI Appendix*, Fig. S4*A*), consistent with the camelina results shown here (*SI Appendix*, Fig. S1*A*) and previous work in pennycress (7). In *fae1* seeds, expression of *EfDAcT* or *EfDAcT+DGAT1 RNAi* resulted in a reduction of 18:3 and an increase in 18:1 compared to the *fae1* control (*SI Appendix*, Fig. S4*B*).

We further confirmed the effect of the *fae1* mutation on acetyl-TAG synthesis by crossing high acetyl-TAG-producing lines expressing *EfDAcT+DGAT1 RNAi* in both *fae1* mutant or wild-type backgrounds with nontransgenic plants of the other background. The cross between *fae1* and *EfDAcT+DGAT1 RNAi* (wild-type) resulted in 82 mol% of acetyl-TAG in seeds homozygous for *fae1* (Fig. 3*C*), higher than the 71 mol% observed in wild-type siblings (Fig. 3*C*). Likewise, the cross between wild-type and *EfDAcT+DGAT1 RNAi* (*fae1*) yielded acetyl-TAG levels of 74 mol% in wild-type segregants, lower than the 96 mol% of acetyl-TAG in seeds homozygous for *fae1* (Fig. 3*C*). These results confirm that the *fae1* mutation increases acetyl-TAG accumulation for plants containing the same transgenic insertion.

***DGAT1* Expression Decreases in Transgenic Pennycress Lines Expressing *EfDAcT*.** To investigate whether the expression of *EfDAcT* in the wild-type or *fae1* mutant background influences genes encoding acyltransferases involved in seed TAG synthesis, we

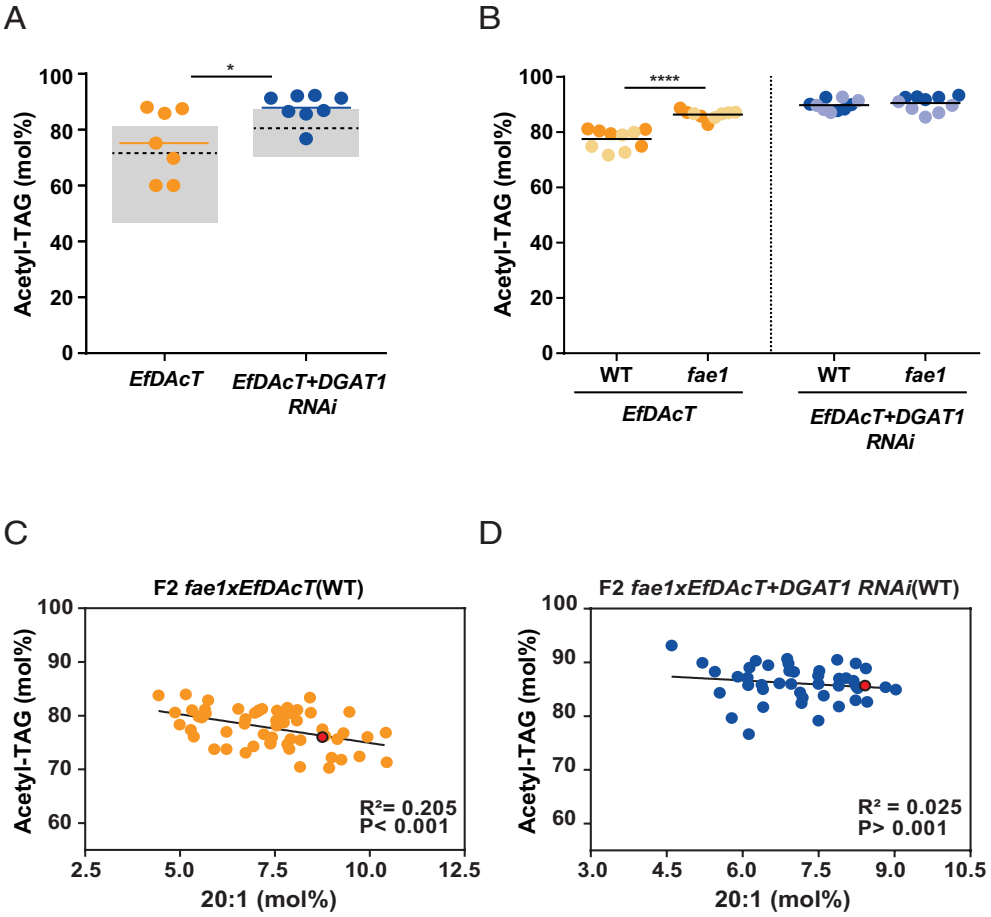

Fig. 2. Mutation of *fae1* has a modest impact on acetyl-TAG accumulation in transgenic camelina lines. (*A*) Scatter plot of acetyl-TAG content in segregating T2 seeds of transgenic *fae1* lines expressing either *EfDAcT* or *EfDAcT+DGAT1 RNAi*. Gray boxes represent previously quantified acetyl-TAG values in wild-type seeds, with the *top and bottom* edges indicating the maximum and minimum values, respectively (10). Horizontal lines represent mean values, n ≥ 3 independent transgenic lines. (*B*) Scatter plot of acetyl-TAG content in homozygous wild-type and *fae1* transgenic lines expressing *EfDAcT* or *EfDAcT+DGAT1 RNAi* that were grown together. Each independent line is represented by a distinct color. Horizontal lines represent mean values, n ≥ 3 biological replicates. Asterisks indicate statistical difference between genotypes (one-way ANOVA followed by Sidak's multiple comparisons test; **P* ≤ 0.05 and *****P* ≤ 0.0001). (*C* and *D*) Linear regression analysis of acetyl-TAG accumulation and 20:1 VLCFA levels in segregating F2 seed from crosses between *fae1* and transgenic wild-type seeds expressing *EfDAcT* (*C*) or *EfDAcT+DGAT1 RNAi* (*D*). The red data point indicates 20:1 and acetyl-TAG accumulation in the original transgenic parent segregating for *EfDAcT* (*C*) or *EfDAcT+DGAT1 RNAi* (*D*). All other data points represent 20:1 and acetyl-TAG content in segregating F2 seed.

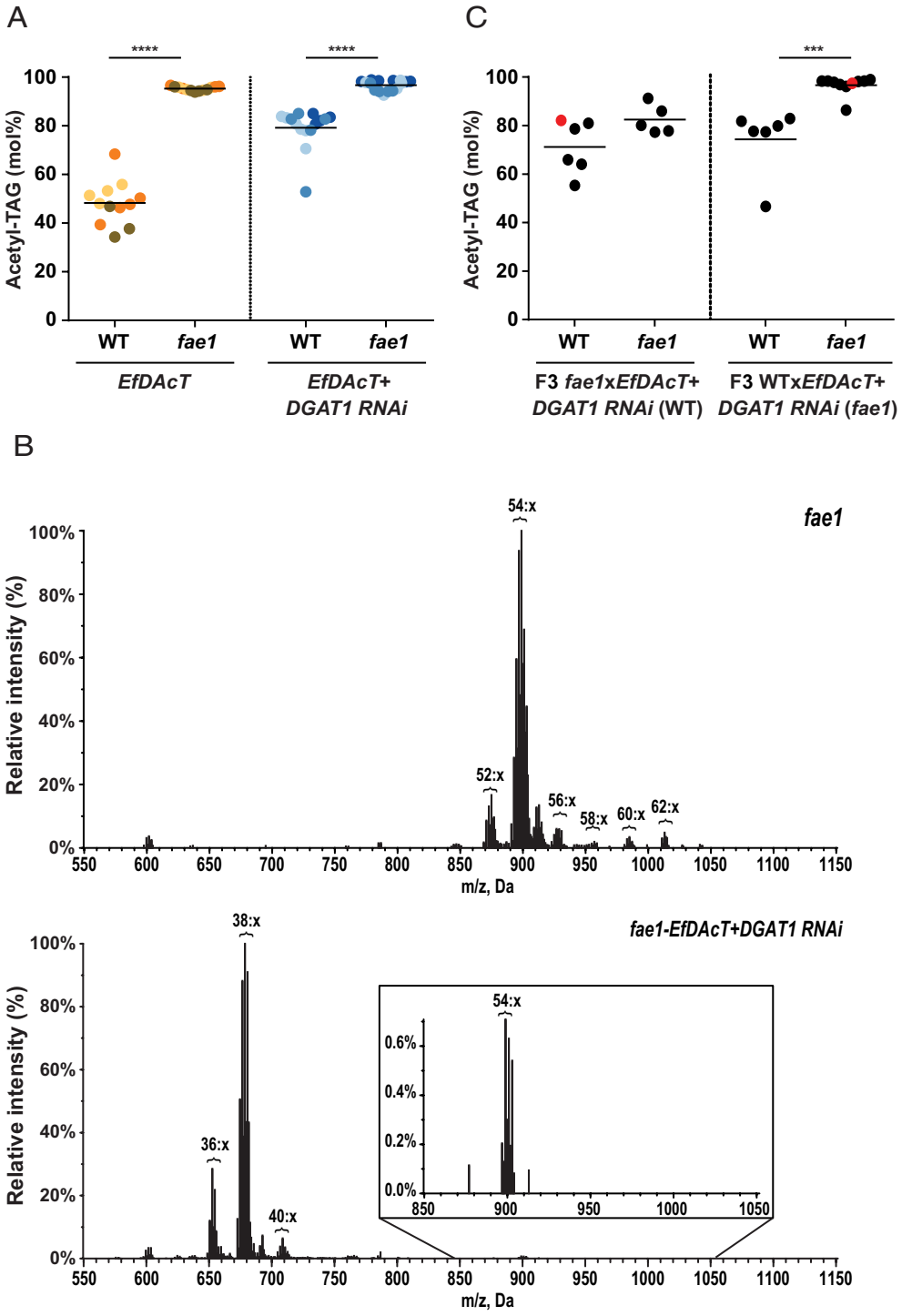

Fig. 3. The *fae1* mutation enhances acetyl-TAG accumulation in transgenic pennycress seeds. (*A*) Scatter plot of acetyl-TAG content in homozygous transgenic wild-type and *fae1* lines expressing *EfDAcT* or *EfDAcT+DGAT1 RNAi*. Each independent line is represented by a distinct color. Horizontal lines represent mean values, n = three independent transgenic lines with ≥3 biological reps. Asterisks indicate statistical difference from wild-type or *fae1* seeds (one-way ANOVA followed by Sidak's multiple comparisons test; ***$P \leq 0.001$ and ****$P \leq 0.0001$). (*B*) Positive ESI-MS spectra of neutral lipids from *fae1* mutant control and homozygous pennycress seeds expressing *EfDAcT+DGAT1 RNAi* in *fae1* background. Signal peaks represent *m/z* values of the $[M + NH_4]^+$ adduct. The number of acyl carbons in each series of acetyl-TAG and TAG molecular species is indicated; the number of double bonds (x) is not delineated. (*C*) Scatter plot of acetyl-TAG levels obtained from homozygous F3 seed crosses between *fae1* or wild-type seeds and transgenic seeds expressing *EfDAcT+DGAT1 RNAi*. Red data points represent acetyl-TAG levels in the transgenic parent used in each cross.

quantified the relative expression of *DGAT1* and *PHOSPHOLIPID DIACYLGLYCEROL ACYLTRANSFERASE1* (*PDAT1*) in the highest acetyl-TAG-producing pennycress lines. The relative expression of *DGAT1* was reduced in the *DGAT1-RNAi* lines as anticipated. Interestingly, in lines expressing only *EfDAcT*, *DGAT1* levels were slightly decreased in the wild-type background and significantly reduced in the *fae1* background (Fig. 4*A*). The *fae1* mutation alone in the nontransgenic control did not impact *DGAT1* expression, suggesting that only the combination of the *fae1* mutation and *EfDAcT* expression had a measurable effect on *DGAT1* expression. In contrast to *DGAT1*, the relative expression of *PDAT1* was not affected by *EfDAcT* expression or the *fae1* mutation (Fig. 4*B*). Analysis of *fae1* mutants showed greatly reduced *FAE1* expression but low levels of transcript were still

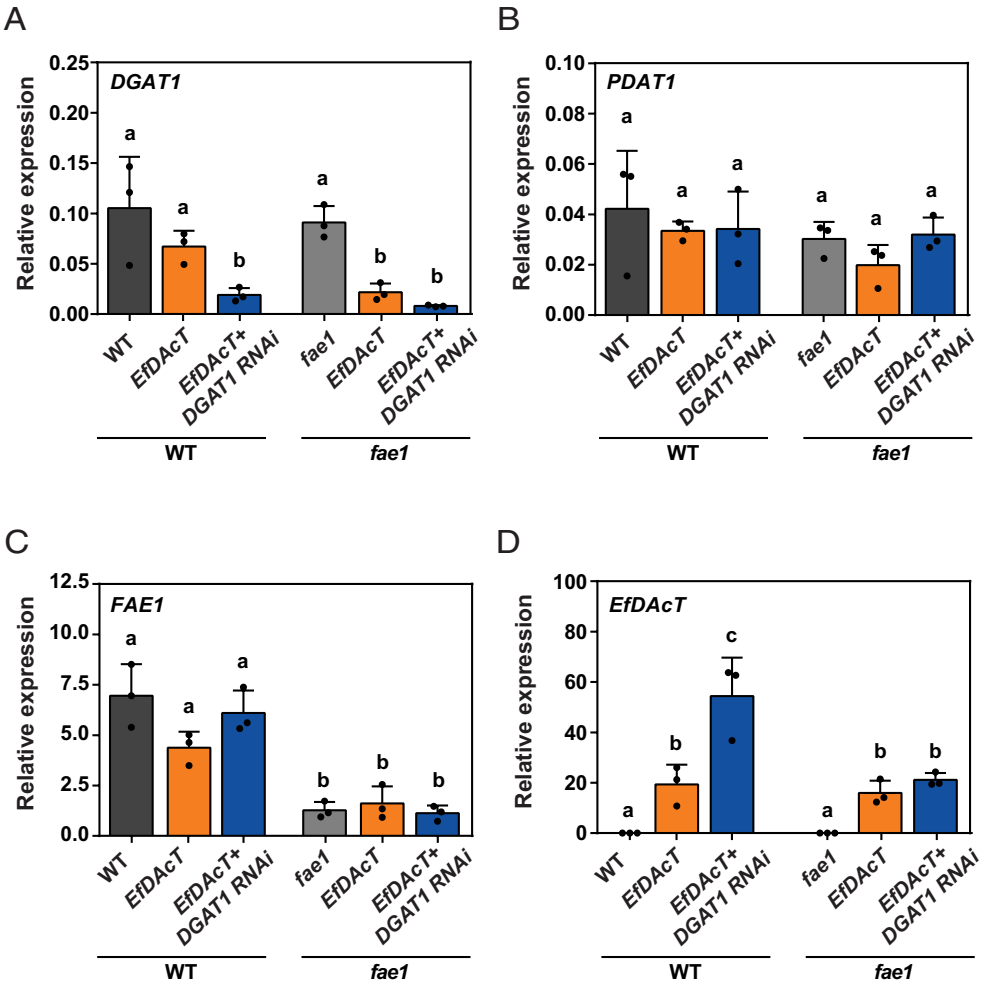

Fig. 4. Assessment of gene expression levels of TAG-related genes in transgenic pennycress lines. Quantitative real-time PCR analysis of *DGAT1* (*A*), *PDAT1* (*B*), *FAE1* (*C*), and *EfDAcT* (*D*) in transgenic wild-type and *fae1* developing seeds expressing *EfDAcT* or *EfDAcT+DGAT1 RNAi* 20 d after flowering. Gene expression levels were normalized to the geometric mean of the reference genes *TIP4* and *UBC*. Data represent mean ± SE, n = 3 biological reps. Different letters indicate statistical difference between genotypes (one-way ANOVA followed by Tukey's multiple comparisons test; $P \leq 0.05$).

detected (Fig. 4*C*). As expected, *EfDAcT* was only expressed in the transgenic lines (Fig. 4*D*), with no apparent correlation between *EfDAcT* expression and acetyl-TAG levels, consistent with our previous findings (10).

Residual TAG in Pennycress Transgenic Seeds Localizes to the Embryonic Axis. Matrix-assisted laser desorption/ionization mass spectrometry (MALDI-MS) imaging was performed on mature pennycress seeds to determine the localization of the acetyl-TAG and residual TAG (Fig. 5). The overall abundance of different molecular species was consistent with the ESI-MS results (*SI Appendix*, Fig. S3). For example, in the wild-type background, the expression of *EfDAcT+DGAT1 RNAi* essentially eliminated the presence of 52:X, 54:X, and 64:X TAG molecular species. Minor variations in the localization of TAG molecular species were noted. In wild-type nontransgenic control seeds, for example, 62:X TAG was more abundant in the cotyledons than in the embryonic axis. Interestingly, 40:X DAG showed a similar distribution pattern (*SI Appendix*, Fig. S4*A*), suggesting a precursor-product relationship, with 40:X DAG being acylated by DGAT1 to produce 62:X TAG. Additionally, 40:X phosphatidylcholine (PC) was absent from the embryonic axis (*SI Appendix*, Fig. S5*B*). With *EfDAcT* expression, 54:X TAG was present in both the cotyledons and the embryonic axis, whereas the less abundant 52:X TAG was only present in the embryonic axis. Strikingly, in *fae1* seeds expressing *EfDAcT+DGAT1 RNAi*, the low amounts of residual TAG (54:X and 52:X TAG) were mostly localized to the embryonic axis.

Acetyl-TAG were present in both the embryonic axis and the cotyledons, though specific molecular species were more abundant in one tissue relative to the other. For example, in the *fae1* background, 38:X acetyl-TAG was lower in the embryonic axis compared to the cotyledons; in contrast, 36:X acetyl-TAG was more abundant in the embryonic axis (Fig. 5). The relative accumulation of these acetyl-TAG molecular species directly corresponds to the levels of their DAG precursor molecules, with 36:X DAG being lower in the embryonic axis compared to the cotyledons, whereas 34:X DAG is more abundant in the embryonic axis (*SI Appendix*, Fig. S5*A*). Interestingly, in nontransgenic *fae1* plants, TAGs derived from these different DAG molecules also possess the same relative accumulation, with 54:X TAG higher in the cotyledons relative to the embryonic axis, and 52:X TAG more abundant in the embryonic axis. These localization results strongly imply that acetyl-TAG and TAG are synthesized from the same tissue-specific DAG pools, consistent with the fact that suppression of DGAT1 increases acetyl-TAG accumulation by reducing competition for the same substrate (4, 10) (Fig. 3).

Acetyl-TAG Production in Transgenic *fae1* Lines Has Minimal Impact on Seed Properties and Plant Growth. In general, all transgenic lines in camelina and pennycress exhibited slight

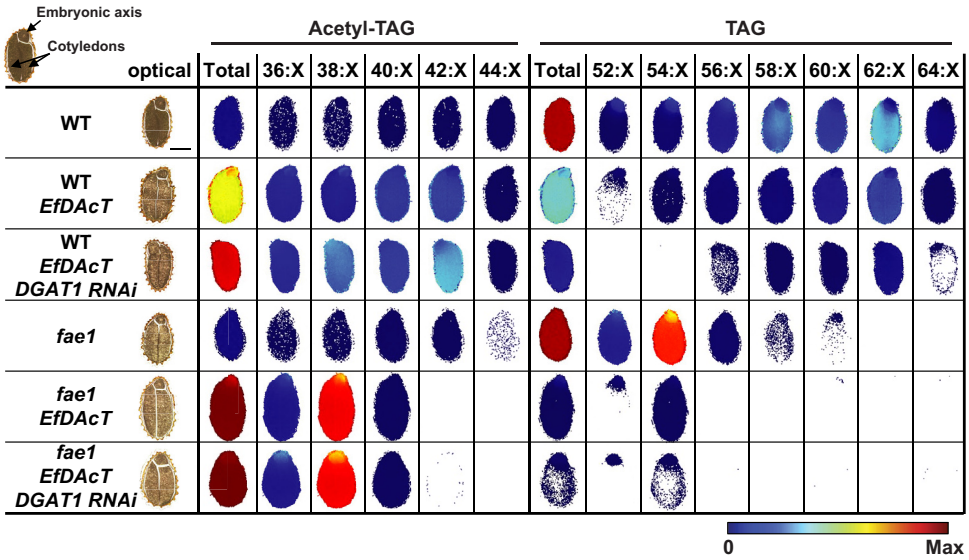

Fig. 5. MALDI-MS imaging of TAG and acetyl-TAG in pennycress mature seeds. MALDI-MS images of TAG potassium adducts $[M + K]^+$ in mature pennycress seeds from wild-type, fae1 mutant, and homozygous pennycress transgenic lines expressing *EfDAcT* or *EfDAcT+DGAT1 RNAi*. Images shown are summed ion images of acetyl-TAG and TAG molecular species with the same number of acyl carbons regardless of the number of double bonds (x). Normalized ion intensities are shown using a jet color scale, with red representing 100% of the total TAG signal. Minimal signals observed as acetyl-TAG for WT and *fae1* are from unknown chemical interferents. The scale bar represents 500 μm. Optical images are included for reference.

increases in total TAG content, seed weight, and seed size compared to the wild-type and *fae1* control lines, while the fatty acid content was slightly reduced (*SI Appendix*, Figs. S6 and S7). Transgenic pennycress lines, particularly those expressing *EfDAcT+DGAT1 RNAi*, exhibited slower germination rates compared to the wild-type and *fae1* control lines (Fig. 6*A* and *SI Appendix*, Fig. S8). The levels of acetyl-TAG in the seeds were very weakly negatively correlated with the germination rate (R^2 = 0.1373), though multiple lines with ultrahigh levels of acetyl-TAG germinated more efficiently than lines with lower levels (*SI Appendix*, Fig. S9). The flowering time for the transgenic *EfDAcT* and *EfDAcT+DGAT1 RNAi* plants was similar to that of nontransgenic controls, with *fae1* plants taking 2 d longer to flower compared to wild-type plants (Fig. 6*B*). The transgenic lines generally exhibited plant heights similar to the wild-type or *fae1* control plants, with the exception of *EfDAcT fae1* plants, which were shorter (Fig. 6*C* and *SI Appendix*, Fig. S10). Although *EfDAcT fae1* plants showed slightly slower growth, this variation in the average flowering time and height was not consistent in other independent lines grown at different times.

Discussion

To enhance acetyl-TAG production in transgenic oilseeds, we optimized endogenous metabolic pathways by eliminating the synthesis of VLCFA and simultaneously suppressing the TAG synthesizing enzyme DGAT1 (Fig. 7). The most successful transgenic lines accumulated 93 mol% acetyl-TAG in camelina seeds and 98 mol% acetyl-TAG in pennycress seeds (Figs. 2*B* and 3 *A* and *B*), higher than previous efforts in transgenic oil seed crops (4, 7, 9, 10) and exceeding levels naturally found in *Euonymus* seeds (1, 3).

Our rationale for blocking VLCFA synthesis was to elevate the levels of acetyl-CoA, a key substrate for EfDAcT-mediated acetyl-TAG synthesis (3, 8). Elimination of VLCFA synthesis showed much larger increases in acetyl-TAG accumulation in pennycress compared to camelina (Figs. 2 and 3). Previous oil engineering studies aiming to enhance accumulation of long-chain polyunsaturated fatty acids (LC-PUFAs) in seeds have also utilized genetic backgrounds defective in VLCFA synthesis. However, consistent with our observed differences between camelina and pennycress, the effect of reducing VLCFA synthesis varies from species to species. For example, efforts to engineer LC-PUFAs in *Brassica carinata* demonstrated significantly higher levels of eicosapentaenoic acid (EPA) in a zero-erucic background compared to in wild-type plants (15). Crossing camelina lines transformed to synthesize LC-PUFAs into a *fae1* background also resulted in significant increases in total LC-PUFA levels (16). However, expression of constructs in *Arabidopsis fae1* mutants led to only minor increases in the accumulation of EPA compared to expression in wild-type plants, though these levels increased in subsequent generations (17). Likewise, although expression of microalgal polyketide synthase-like PUFA synthase system in *Arabidopsis* resulted in lower levels of endogenous VLCFA, consistent with competition between fatty acid elongation and PUFA synthesis, subsequent experiments expressing the PUFA synthase system in a *fae1* mutant background did not result in higher LC-PUFA accumulation (18). These differing results indicate that more needs to be learned about the flux of fatty acids from synthesis into storage oils, particularly in a species-specific context, in order to more rationally alter oil composition.

In our study, we observed much larger increases in acetyl-TAG accumulation in pennycress compared to camelina when VLCFA synthesis was eliminated. Wild-type pennycress contains more than 50 mol% of VLCFAs, notably higher than the approximately 26 mol% found in camelina (Fig. 1*A*), explaining why pennycress and not camelina *fae1* seeds possess much higher acetyl-CoA levels compared to wild-type controls (Fig. 1*E*). These higher levels of acetyl-CoA are one likely explanation for why larger increases in acetyl-TAG accumulation were observed in pennycress when *FAE1* is mutated. However, other nonexclusive mechanisms could also explain the particularly large increases in acetyl-TAG accumulation in the *fae1* pennycress mutant. For example, the removal of VLCFA might prevent the efficient functioning of pennycress DGAT1 to synthesize TAG. In Brassicaceae species, the majority of VLCFA at the *sn*-3 position of TAG are the result of DGAT1 activity (19, 20), suggesting that the increase of acetyl-TAG in pennycress *fae1* mutants might be caused by EfDAcT

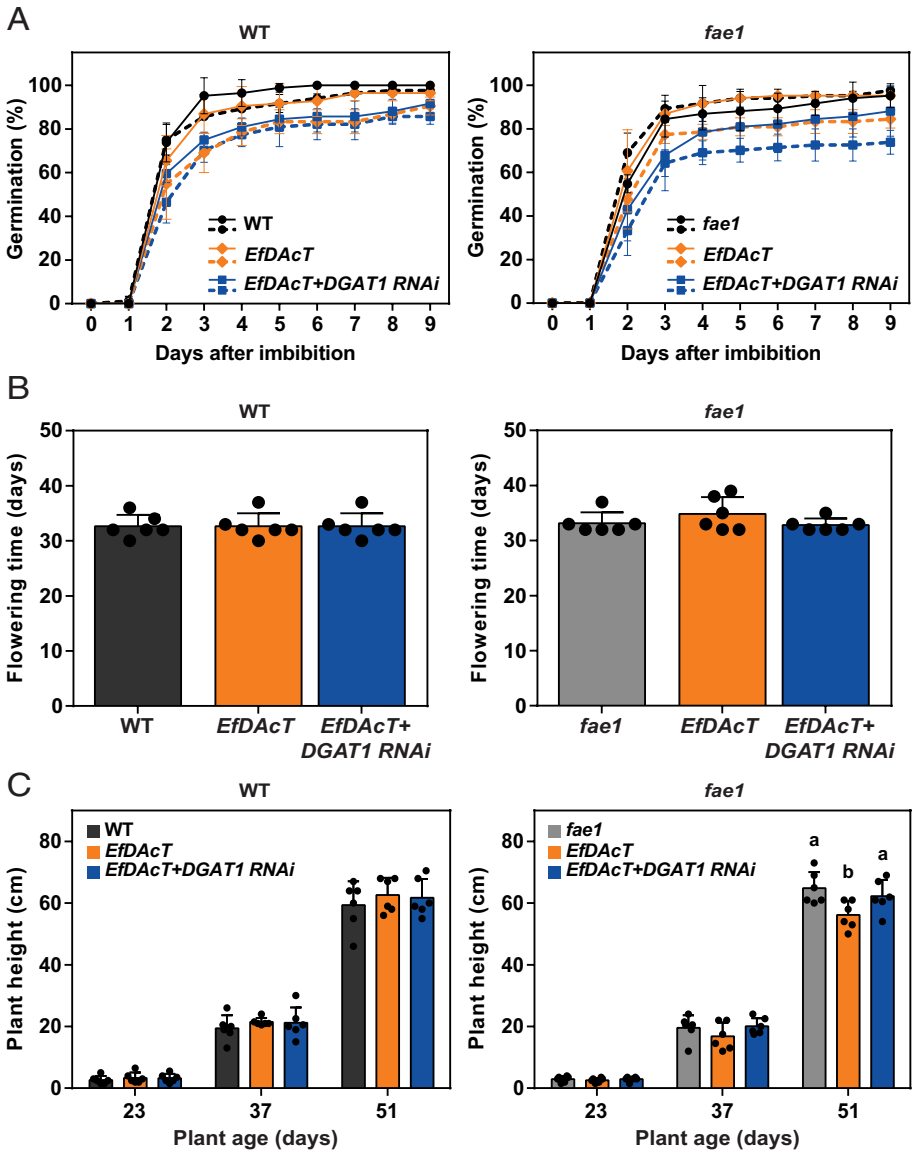

Fig. 6. Seed germination and plant traits of pennycress high acetyl-TAG-producing lines. (*A*) Germination rates of seed from homozygous transgenic lines expressing *EfDAcT* or *EfDAcT+DGAT1 RNAi* in both wild-type and *fae1* backgrounds. Solid and dashed lines indicate different independent lines. Data represent mean ± SE, n = 3 biological replicates. (*B*) Time in days until first flower opening. (*C*) Plant height measurements at 21, 37, and 51 d after planting. Data represent mean ± SE of two independent transgenic lines with three biological replicates. Different letters indicate statistical difference between genotypes (one-way ANOVA followed by Tukey's multiple comparisons test; $P \leq 0.05$).

outcompeting DGAT1 due to absence of the VLCFA substrates utilized by DGAT1. We also observed that *DGAT1* expression was reduced when *EfDAcT* was expressed, with much greater suppression in the *fae1* background (Fig. 4*A*), enabling synthesis of acetyl-TAG via EfDAcT to outcompete that of endogenous TAG via DGAT1 in the *fae1* background. While the mechanism mediating this decrease in *DGAT1* expression is currently unknown, it is tempting to speculate that *DGAT1* gene expression is somehow regulated by DGAT1 activity itself and is reduced due to lack of VLCFA substrate.

All transgenic lines accumulated acetyl-TAG in the cotyledons and the embryonic axis (Fig. 5), indicating that EfDAcT can acetylate DAG molecular species in both tissues. *FAE1* expression has been demonstrated to be predominantly concentrated in the cotyledons as opposed to the embryonic axis (21, 22), which may underlie the preferential distribution of PC, DAG, and TAGs containing VLCFAs to the cotyledonary tissues. In the *fae1* mutant background, most of the residual TAG (~2 to 4 mol%) localizes to the embryonic axis (Fig. 5), suggesting that *DGAT1-RNAi* and *EfDAcT* might more effectively target or compete with endogenous TAG-synthesizing enzymes in the cotyledonary tissues compared to the embryonic axis. This raises the possibility that employing tissue-specific promoters to express *EfDAcT* and to suppress endogenous TAG- acyltransferases within the embryonic axis could offer another strategy to eliminate the remaining residual TAG.

Engineering unusual lipids in oilseeds has typically affected seed characteristics and decreased oil levels (23–25). The accumulation of ~98 mol% of acetyl-TAG in transgenic pennycress seeds has no major impact on plant growth, as no significant morphological differences were observed between transgenic plants and the wild-type or *fae1* control plants (*SI Appendix*, Fig. S10 and Fig. 6 *B* and *C*). Total TAG, seed weight, and seed size were slightly increased and total fatty acid content was slightly reduced in both camelina and pennycress transgenic seeds (*SI Appendix*, Figs. S6 and S7), similar to previous results (4, 10). The higher levels of total TAG are likely caused by the absence of an acyl chain at the *sn*-3 position of acetyl-TAG, which promotes an increased availability of free fatty acids for further integration into additional TAG

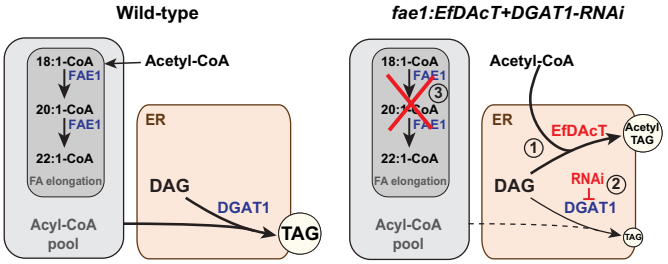

Fig. 7. Strategies for engineering ultrahigh levels of acetyl-TAG in camelina and pennycress. In wild-type seeds, TAGs are mostly produced through the activity of DGAT1, which transfers an acyl group to the *sn*-3 position of DAG to produce TAG. To engineer ultrahigh levels of acetyl-TAG in transgenic plants, multiple strategies were used including 1) the expression of a high-activity acetyltransferase (EfDAcT) which transfers an acetate group from acetyl-CoA to the *sn*-3 position of DAG to produce acetyl-TAG; 2) RNAi to inhibit DGAT1 expression and reduce TAG synthesis; and 3) mutating *FAE1* to increase acetyl-CoA levels available for EfDAcT. In pennycress, the absence of VLCFA in the acyl-CoA pool caused by *fae1* mutation could also reduce the ability of DGAT1 to use the remaining acyl-CoA, as illustrated by the dashed arrow. Abbreviations: Acetyl-TAG, acetyl-triacylglycerol; DAG, diacylglycerol; DGAT1, diacylglycerol acyltransferase1; EfDAcT, *Euonymus fortunei* diacylglycerol acetyltransferase; FAE1, fatty acid elongase1; RNAi, RNA interference; TAG, triacylglycerol.

glycerol backbones (4, 10). However, an increased availability of fatty acids, if not rapidly incorporated into TAG molecules, causes feedback inhibition of de novo fatty acid synthesis (26, 27), likely accounting for the slight reduction in the overall fatty acid content observed in the transgenic lines (*SI Appendix*, Figs. S6*B* and S7*B*). Pennycress transgenic seeds also exhibited reduced germination rates (Fig. 6*A*), similar to previous results in camelina (10). The cause of reduced germination in transgenic seeds accumulating acetyl-TAG remains unclear as germination is a highly complex trait regulated by numerous processes (28). Future experiments are needed to examine whether acetyl-TAG accumulation impacts any of these activities, altering germination rates.

In summary, we have successfully generated transgenic lines that mimic or exceed the natural production levels of acetyl-TAG found in native species, providing economically viable sources of low-viscosity oil for potential applications across various industries. Our results provide evidence that native-like levels of unusual TAGs can be produced in transgenic oilseed crops through the coordinated expression of the most efficient biosynthetic genes, ensuring the presence of suitable substrates by manipulating the fatty acid composition of the host plant, and eliminating competitive metabolic pathways. Such results underscore the feasibility of engineering designer lipids with extreme fatty acid compositions at near quantitative levels that are a crucial goal if sustainable fuels from plants are to be achieved at high levels in a cost-effective way.

Methods

Plant Material and Growth Conditions. The following ecotypes were used in this study: camelina "Suneson" and pennycress "Spring-32." CRISPR-generated *fae1* mutant camelina and pennycress seeds have been described previously (7, 13). Plants were grown on soil (4:2:1 mixture of Berger BM6 All-Purpose soil mix:vermiculite:perlite) in growth chambers under a 16 h light/8 h dark cycle at a light intensity of 250 μmol m^{-2} s^{-1}, and a temperature of 21 °C. To obtain developing seeds for metabolite and RT-qPCR analysis, emerging flowers were tagged using colored threads. Tagged pods were harvested at 20 DAF (days after flowering), immediately frozen in liquid nitrogen, and stored at −80 °C until further analysis.

Generation of Transgenic Plants. Plasmids containing *EfDAcT* and *EfDAcT+DGAT1-RNAi* (10, 29) were introduced into *Agrobacterium tumefaciens* strain GV3101 and transformed into wild-type and *fae1* mutants camelina and pennycress plants via a floral dip vacuum infiltration method (7, 30). Transgenic seeds were identified by visual screening for DsRed in mature seeds for camelina and in seedlings for pennycress due to its dark seed coat (7, 10).

Generation of Crosses and Genotyping of Transgenic *fae1* Mutant Lines. Crosses were generated by transferring pollen from a mature flower of the transgenic male donor onto the stigma of the emasculated maternal plants (wild-type or *fae1*). Successful F1 crosses were identified by visual screening for DsRed and propagated to the F2 generation. Segregating F2 camelina seeds expressing DsRed were directly used for lipid analysis. F2 pennycress seeds positive for DsRed were propagated to the F3 generation to identify plants homozygous for EfDAcT (DsRed screening) and the *fae1* mutation. Genotyping for *fae1* was performed using derived cleaved amplified polymorphic sequence analysis (dCAPS) (31) as illustrated in *SI Appendix*, Fig. S11. Genomic DNA was extracted from leaves as previously described (32). Genotyping primers are listed in *SI Appendix*, Table S1.

Lipid Analysis. Total lipids were extracted from mature seeds using a hexane–isopropanol-based method (33). One hundred micrograms of tri 15:0-TAG (NuChek Prep, New Elysian, MN) was added as an internal standard during lipid extraction. For quantification of acetyl-TAG/TAG content and FA composition, total lipid extracts were loaded onto thin layer chromatography silica gel 60 plates for separation with a 70:30:1 hexane:diethyl ether:acetic acid (v/v/v) solvent system. TAG and acetyl-TAG bands were scraped and subjected to acid-catalyzed transesterification (33). Fatty acid methyl esters (FAMEs) extracts were analyzed on a DB23 column, using a Shimadzu GC-2010 plus gas chromatograph with a flame ionization detector (FID) (34). Acetyl-TAG and TAG levels were calculated as described previously (4). For ESI-MS analysis, neutral lipids were collected by passage of total lipid extracts over a small silica column with 99:1 (v/v) chloroform:methanol. Neutral lipid samples were analyzed on an electrospray ionization triple quadrupole mass spectrometer (Sciex QTRAP 6500+, Sciex, Framingham, MA) (35). The total FA content of mature seeds was determined by homogenizing 20 seeds in 1 ml toluene with a PT2500E polytron (Kinematica AGd) followed by transesterification and gas chromatography as stated above.

Analysis of Seed Properties and Plant Growth. Seed weight was determined by weighing 100 dry seeds on a Sartorius CP225D analytical balance. The seed size of ~200 randomly chosen seeds was calculated utilizing ImageJ software, using a well-established method (36). Germination assays were performed as previously described (10). Mature seeds were surface-sterilized and planted on 1% agar plates. Plates were placed in a growth chamber, and germination was scored daily for 9 d. Plant growth phenotypes were analyzed in transgenic plants grown alongside wild-type and *fae1* mutants. Flowering time, measured in days after planting, was determined when the first inflorescence appeared at any node in the main stem. Plant height was determined at 23, 37, and 51 d after planting by measuring the distance from the soil surface to the highest point of the main stem.

Acetyl-CoA Quantification. Metabolites were extracted from ~100 mg (fresh weight) camelina seeds as previously described (37) using 1,200 μL cold (−20 °C) methanol:chloroform solution (7:3 v/v), 480 μL chilled (4 °C) double-distilled water, and internal standards (PIPES, norvaline, and ribitol). The upper polar phase was vacuum dried in a SpeedVac overnight at 8 °C, resuspended with 50 μL of 50% methanol with 0.2% formic acid, and passed through a 0.45-μm centrifugal filter (Costar, Corning Inc.). Samples were analyzed by LC-MS/MS using a Shimadzu HPLC system (UFLC-XR; Shimadzu Corporation, Kyoto, Japan) connected to an electrospray ionization triple-quadrupole MS (Sciex QTRAP 6500). Metabolites were separated on an Imtakt Intrada organic acid column (150 × 2 mm, 3 μm; Kyoto, Japan) and detected in negative ion mode following previously described methods and MS parameters (38). For quantification of pool sizes, metabolite concentrations and recoveries were calculated based on calibration curves of the individual standard and the internal standard ribitol, respectively.

MALDI-MSI Sample Preparation and Data Acquisition. Desiccated seeds were lightly fixed using slight modifications of a previously published method (39). Briefly, a 50 mM PIPES buffer, adjusted to a pH of 7.2 with potassium hydroxide, was prepared. Desiccated seeds were placed in a 4% (w/v) formaldehyde in the PIPES buffer and allowed to sit in the solution for 30 min. Excess fixative was washed

with three successive 5-min PIPES buffer washes. The lightly fixed seeds were then embedded in 10% w/v gelatin, flash-frozen using liquid nitrogen, and equilibrated to −20 °C in a freezer for at least 8 h. The embedded seeds were sectioned to a 20 μm thickness at −20 °C using a cryomicrotome (Leica CM1850, Leica Microsystems; Buffalo Grove, IL), collected on Cryo-Jane tape (Leica Biosystems; Wetzlar, Germany), and then mounted onto glass slides. After sectioning, slides were stored at −80 °C until sample preparation. Samples were placed on a −80 °C prechilled aluminum block and lyophilized under vacuum for 1.25 h. After drying, tissue integrity was checked under a microscope, and optical images were obtained using a BX53 microscope (Olympus; Shinjuku City, Tokyo, Japan). Next, 6.5 mM potassium acetate in methanol was applied using a TM sprayer (HTX Technologies; Chapel Hill, NC). A flow rate of 0.03 mL/min was used for a total of eight passes with 3 mm spacing in a crisscross pattern at a velocity of 1,200 mm/min with a nitrogen gas pressure of 10 psi and nozzle temperature of 30 °C. 2,5-dihydroxyacetophenone (DHAP) in 90:10 acetonitrile:water (20 mg/mL) was sprayed onto the sample surface as a matrix using the TM sprayer (flow rate of 0.10 mL/min, sixteen passes, 3 mm spacing, crisscross pattern, a velocity of 1,200 mm/min, nitrogen gas pressure of 10 psi, and nozzle temperature of 30 °C). Gold was then sputtered on top of the sample for 20 s at 40 mA using a Cressington 108 auto Sputter Coater (Ted Pella; Redding, CA). Mass spectral data were acquired using a high-resolution mass spectrometer (Q Exactive HF Orbitrap, Thermo Scientific; San Jose, CA), equipped with a Spectroglyph MALDI source (Kennewick, WA). All experiments were performed using a mass resolution of 120,000 at *m/z* 200, maximum injection time of 250 ms, *m/z* range of 500 to 1,200, and a raster step of 20 μm. Data were analyzed using Xcalibur (Thermo Scientific, V4.2.47), Image Insight (Spectroglyph), and MSiReader (North Carolina State University; Raleigh, NC) software. All mass spectrometry images were generated with a ±10 ppm mass tolerance due to mass drift across datasets.

RT-qPCR Analysis. Total RNA was isolated from 15 pooled pennycress developing seeds using the RNAqueous Total RNA Isolation Kit (Ambion, Austin, TX) followed by lithium chloride precipitation according to the manufacturer's instructions. Total RNA was digested with the TURBO DNA-*free* Kit (Invitrogen, Carlsbad, CA) to remove any genomic DNA contamination. RNA concentrations were quantified with a NanoDrop 2000 spectrophotometer (Thermo Scientific; San Jose, CA). One microgram of total RNA was used for cDNA synthesis using the iScript cDNA Synthesis kit (Bio-Rad, Hercules, CA). Quantitative PCR was performed on a CFX96 real-time PCR system (Bio-Rad) using iTAQ Universal SYBR Green Supermix (Bio-Rad) following the manufacturer's guidelines. mRNA levels were normalized to the geometric mean of the reference genes *UBC21* and *TIP41* using the $2^{-\Delta Ct}$ method (40). Primers used for RT-qPCR are listed in *SI Appendix*, Table S1.

Data, Materials, and Software Availability. All study data are included in the article and/or *SI Appendix*.

ACKNOWLEDGMENTS. This work was supported by the United States Department of Agriculture–National Institute of Food and Agriculture under award number 2020-67013-30897 to Y.-J.L. and T.P.D., award numbers 2018-67009-27374 and 2019-69012-29851 to J.C.S., and the Hatch/Multi-State project 1013013 to T.P.D., by the United States Department of Agriculture–Agriculture Research Service support to D.K.A., by the U.S. Department of Energy, Office of Science, Office of Biological & Environmental Research, under Award Number DE-SC0023142 to C.L., D.K.A., and T.P.D., by the NSF Division of Integrative Organismal Systems award number 1829365 in support of S.K., and a Saudi Arabian Cultural Mission fellowship to L.A. The lipidomics analyses described in this work were performed at the Kansas Lipidomics Research Center Analytical Laboratory. Instrument acquisition and lipidomics method development were supported by the NSF (including support from the Major Research Instrumentation program; most recent award DBI-1726527), K-IDeA Networks of Biomedical Research Excellence of National Institute of Health (P20GM103418), and Kansas State University. The Danforth Center Proteomics and Mass Spectrometry Facility is acknowledged for use of instrumentation including a Quadrupole-Trap Liquid Chromatography-Tandem Mass Spectrometer 6500 acquired through the NSF under grant number DBI-1427621. Portions of the paper were developed from the dissertation of L.A. Contribution no. 24-206-J from the Kansas Agricultural Experiment Station.

Author affiliations: [a]Department of Biochemistry and Molecular Biophysics, Kansas State University, Manhattan, KS 66506; [b]Division of Biology, Kansas State University, Manhattan, KS 66506; [c]School of Biological Sciences, Illinois State University, Normal, IL 61790; [d]Department of Chemistry, Iowa State University, Ames, IA 50011; [e]Donald Danforth Plant Science Center, St. Louis, MO 63132; [f]Department of Plant Sciences and Plant Pathology, Montana State University, Bozeman, MT 59717; and [g]United States Department of Agriculture, Agricultural Research Service, St. Louis, MO 63132

1. R. Kleiman, R. W. Miller, F. R. Earle, I. A. Wolff, *(S)*-1,2-diacyl-3-acetins: Optically active triglycerides from *Euonymus verrucosus* seed oil. *Lipids* **2**, 473–478 (1967).
2. R. A. Sidorov, A. V. Zhukov, V. P. Pchelkin, A. G. Vereshchagin, V. D. Tsydendambaev, Content and fatty acid composition of neutral acylglycerols in *Euonymus* fruits. *J. Am. Oil Chem. Soc.* **91**, 805–814 (2014).
3. T. P. Durrett *et al.*, A distinct DGAT with *sn*-3 acetyltransferase activity that synthesizes unusual, reduced-viscosity oils in *Euonymus* and transgenic seeds. *Proc. Natl. Acad. Sci. U.S.A.* **107**, 9464–9469 (2010).
4. J. Liu *et al.*, Metabolic engineering of oilseed crops top produce high levels of novel acetyl glyceride oils with reduced viscosity, freezing point and calorific value. *Plant Biotechnol. J.* **13**, 858–865 (2015).
5. S. Bansal, T. P. Durrett, *Camelina sativa*: An ideal platform for the metabolic engineering and field production of industrial lipids. *Biochimie* **120**, 9–16 (2016).
6. M. R. Malik *et al.*, *Camelina sativa*, an oilseed at the nexus between model system and commercial crop. *Plant Cell Rep.* **37**, 1367–1381 (2018).
7. M. McGinn *et al.*, Molecular tools enabling pennycress (*Thlaspi arvense*) as a model plant and oilseed cash cover crop. *Plant Biotechnol. J.* **17**, 776–788 (2019).
8. S. Bansal, T. P. Durrett, Defining the extreme substrate specificity of *Euonymus alatus* diacylglycerol acetyltransferase, an unusual membrane-bound O-acyltransferase. *Biosci. Rep.* **36**, e00406 (2016).
9. J. Liu *et al.*, Field production, purification and analysis of high-oleic acetyl-triacylglycerols from transgenic *Camelina sativa*. *Ind. Crops. Prod.* **65**, 259–268 (2015).
10. L. Alkotami *et al.*, Expression of a high-activity diacylglycerol acetyltransferase results in enhanced synthesis of acetyl-TAG in camelina seed oil. *Plant J.* **106**, 953–964 (2021).
11. D. W. James Jr. *et al.*, Directed tagging of the arabidopsis *FATTY ACID ELONGATION1* (*FAE1*) gene with the maize transposon activator. *Plant Cell* **7**, 309–319 (1995).
12. L. Kunst, D. C. Taylor, E. W. Underhill, Fatty acid elongation in developing seeds of *Arabidopsis thaliana*. *Plant Physiol. Bioch.* **30**, 425–434 (1992).
13. M. E. Ozseyhan, J. Kang, X. Mu, C. Lu, Mutagenesis of the *FAE1* genes significantly changes fatty acid composition in seeds of *Camelina sativa*. *Plant Physiol. Bioch.* **123**, 1–7 (2018).
14. C. Hutcheon *et al.*, Polyploid genome of *Camelina sativa* revealed by isolation of fatty acid synthesis genes. *BMC Plant Biol.* **10**, 233 (2010).
15. B. Cheng *et al.*, Towards the production of high levels of eicosapentaenoic acid in transgenic plants: The effects of different host species, genes and promoters. *Transgenic Res.* **19**, 221–229 (2010).
16. L. Han, R. P. Haslam, S. Silvestre, C. Lu, J. A. Napier, Enhancing the accumulation of eicosapentaenoic acid and docosahexaenoic acid in transgenic Camelina through the CRISPR-Cas9 inactivation of the competing pathway. *Plant Biotechnol. J.* **20**, 1444–1446 (2022).
17. N. Ruiz-Lopez, R. P. Haslam, S. L. Usher, J. A. Napier, O. Sayanova, Reconstitution of EPA and DHA biosynthesis in Arabidopsis: Iterative metabolic engineering for the synthesis of n−3 LC-PUFAs in transgenic plants. *Metab. Eng.* **17**, 30–41 (2013).
18. T. A. Walsh *et al.*, Canola engineered with a microalgal polyketide synthase-like system produces oil enriched in docosahexaenoic acid. *Nat. Biotechnol.* **34**, 881–887 (2016).
19. V. Katavic *et al.*, Alteration of seed fatty acid composition by an ethyl methanesulfonate-induced mutation in *Arabidopsis thaliana* affecting diacylglycerol acyltransferase activity. *Plant Physiol.* **108**, 399–409 (1995).
20. H. K. Woodfield *et al.*, Using lipidomics to reveal details of lipid accumulation in developing seeds from oilseed rape (*Brassica napus* L.). *Biochim. Biophys. Acta Mol. Cell Biol. Lipids* **1863**, 339–348 (2018).
21. S. Lu, M. Aziz, D. Sturtevant, K. D. Chapman, L. Guo, Heterogeneous distribution of erucic acid in *Brassica napus* seeds. *Front. Plant Sci.* **10**, 1744 (2020).
22. M. Rossak, M. Smith, L. Kunst, Expression of the *FAE1* gene and *FAE1* promoter activity in developing seeds of *Arabidopsis thaliana*. *Plant Mol. Biol.* **46**, 717–725 (2001).
23. M. Esfahanian *et al.*, Generating pennycress (*Thlaspi arvense*) seed triacylglycerols and acetyl-triacylglycerols containing medium-chain fatty acids. *Front. Energy Res.* **10**, 620118 (2021).
24. D. Lunn, G. A. Smith, J. G. Wallis, J. Browse, Development defects of hydroxy-fatty acid-accumulating seeds are reduced by castor acyltransferases. *Plant Physiol.* **177**, 553–564 (2018).
25. A. R. Snapp, J. Kang, X. Qi, C. Lu, A fatty acid condensing enzyme from *Physaria fendleri* increases hydroxy fatty acid accumulation in transgenic oilseeds of *Camelina sativa*. *Planta* **240**, 599–610 (2014).
26. C. Andre, R. P. Haslam, J. Shanklin, Feedback regulation of plastidic acetyl-CoA carboxylase by 18:1-acyl carrier protein in *Brassica napus*. *Proc. Natl. Acad. Sci. U.S.A.* **109**, 10107–10112 (2012).
27. P. D. Bates *et al.*, Fatty acid synthesis is inhibited by inefficient utilization of unusual fatty acids for glycerolipid assembly. *Proc. Natl. Acad. Sci. U.S.A.* **111**, 1204–1209 (2014).
28. M. Koornneef, L. Bentsink, H. Hilhorst, Seed dormancy and germination. *Curr. Opin. Plant Biol.* **5**, 33–36 (2002).
29. T. N. T. Tran, J. Shelton, S. Brown, T. P. Durrett, Membrane topology and identification of key residues of *Ea*DAcT, a plant MBOAT with unusual substrate specificity. *Plant J.* **92**, 82–94 (2017).
30. C. Lu, J. Kang, Generation of transgenic plants of a potential oilseed crop *Camelina sativa* by *Agrobacterium*-mediated transformation. *Plant Cell Rep.* **27**, 273–278 (2008).
31. M. M. Neff, J. D. Neff, J. Chory, A. E. Pepper, dCAPS, a simple technique for the genetic analysis of single nucleotide polymorphisms: Experimental applications in *Arabidopsis thaliana* genetics. *Plant J.* **14**, 387–392 (1998).
32. K. Edwards, C. Johnstone, C. Thompson, A simple and rapid method for the preparation of plant genomic DNA for PCR analysis. *Nucleic Acids Res.* **19**, 1349 (1991).

33. Y. Li, F. Beisson, M. Pollard, J. Ohlrogge, Oil content of Arabidopsis seeds: The influence of seed anatomy, light and plant-to-plant variation. *Phytochemistry* **67**, 904–915 (2006).
34. J. A. Aznar Moreno, T. P. Durrett, Simultaneous targeting of multiple gene homeologues to alter seed oil production in *Camelina sativa*. *Plant Cell Physiol.* **58**, 1260–1267 (2017).
35. S. Bansal, T. P. Durrett, Rapid quantification of low-viscosity acetyl-triacylglycerols using electrospray ionization mass spectrometry. *Lipids* **51**, 1093–1102 (2016).
36. R. P. Herridge, R. C. Day, S. Baldwin, R. C. Macknight, Rapid analysis of seed size in Arabidopsis for mutant and QTL discovery. *Plant Methods* **7**, 1–11 (2011).
37. F. Ma, L. J. Jazmin, J. D. Young, D. K. Allen, "Isotopically nonstationary metabolic flux analysis (INST-MFA) of photosynthesis and photorespiration in plants" in *Photorespiration: Methods and Protocols*, A. R. Fernie, H. Bauwe, A. P. M. Weber, Eds. (Humana Press, New York, NY, 2017), pp. 167–194.
38. S. Koley, K. L. Chu, S. S. Gill, D. K. Allen, An efficient LC–MS method for isomer separation and detection of sugars, phosphorylated sugars, and organic acids. *J. Exp. Bot.* **73**, 2938–2952 (2021).
39. P.J. Horn *et al.*, Spatial mapping of lipids at cellular resolution in embryos of cotton. *Plant Cell*, **24**, 622-636 (2012).
40. K. J. Livak, T. D. Schmittgen, Analysis of relative gene expression data using real-time quantitative PCR and the $2-\Delta\Delta CT$ method. *Methods* **25**, 402–408 (2001).